Bulletin of the Seismological Society of America, Vol. 87, No. 2, pp. 463–473, April 1997

The Kozani–Grevena (Greece) Earthquake of 13 May 1995 Revisited from a Detailed Seismological Study

by D. Hatzfeld, V. Karakostas, M. Ziazia, G. Selvaggi, S. Leborgne, C. Berge, R. Guiguet, A. Paul, P. Voidomatis, D. Diagourtas, I. Kassaras, I. Koutsikos, K. Makropoulos, R. Azzara, M. Di Bona, S. Baccheschi, P. Bernard, and C. Papaioannou

Abstract The Kozani earthquake (M_s = 6.6) of 13 May 1995 is the strongest event of the decade in Greece and occurred in a region of low seismic activity. Using regional data and the strong-motion record at the Kozani station, we relocate the mainshock at 40.183° N and 21.660° E, beneath the Vourinos massif at a depth of 14.2 km. We also compute a focal mechanism by body-waveform modeling at teleseismic distance, which confirms a normal mechanism. The most likely plane strikes 240° ± 1° N and dips 40° ± 1° N with a centroid depth of 11 ± 1 km. Modeling of the strong-motion record at Kozani confirms that nucleation started at the eastern termination of the bottom of the fault.

Six days after the mainshock, we installed a network of 40 portable seismological stations for one week around the epicentral region. Several thousand aftershocks were recorded, among which we locate 622 with a precision better than 1 km. We compute 181 focal mechanisms that mostly show normal faulting. The aftershock seismicity is restricted between 5 and 15 km depth and defines a plane dipping north at an angle of about 35°, consistent with the mainshock mechanism. Seismic activity with the same pattern of normal fault mechanisms is also seen on an antithetic fault connected to the main one at 12 km depth, which cuts the ground surface north of the Vourinos ophiolite massif in the Siatista valley. These results suggest two possibilities for the active fault plane; either it is the Deskati fault that is flat and dips with a constant angle, and therefore the surface breaks are secondary features, or, more likely, it is the Paleohori fault that is new, of listric shape, and located ahead of the Deskati fault, which was not active during the earthquake.

Introduction

On 13 May 1995 an earthquake of magnitude M_s = 6.6 occurred in Northern Greece and severely damaged about 5000 houses. This earthquake was "unexpected" in the sense that the epicentral region was assumed to be of low seismic risk (Papazachos *et al.*, 1995; Stiros, 1995).

The seismicity of the Aegean is the highest in western Europe and is the most striking evidence for the complex and intense active tectonics of the region (Fig. 1). Most of the activity is located along the Hellenic trench and in western Greece and is related to the active convergent boundary between the Aegean and the African plates in the south and to the continental collision between Apulia and the Aegean in the west. Within the Aegean, seismicity is related to the western termination of the North Anatolian fault or to a few extensional structures such as the Gulf of Corinth or Central Greece. An instrumental seismicity map clearly shows active deformation in most of the Aegean with only two relatively quiet regions: the Sea of Crete and northern Thessaly.

Identification of potential seismic sources is important for earthquake hazard mitigation. Assuming that earthquakes occur periodically at the same place, seismicity maps, historical catalogs, and maps of active faults are the information used to infer the seismic hazard in a region. The unexpected Kozani earthquake will certainly modify the view of the tectonics and the seismic hazard in Greece (Stiros, 1995). The original location of this event motivated the deployment of a dense network of portable seismological stations. The results of the aftershock study are presented here as well as a detailed examination of the characteristics of the mainshock. Preliminary seismological results have already been given by Papazachos *et al.* (1995) and Hatzfeld *et al.* (1995), suggesting a normal faulting earthquake on a fault striking NE–SW and dipping toward the NW.

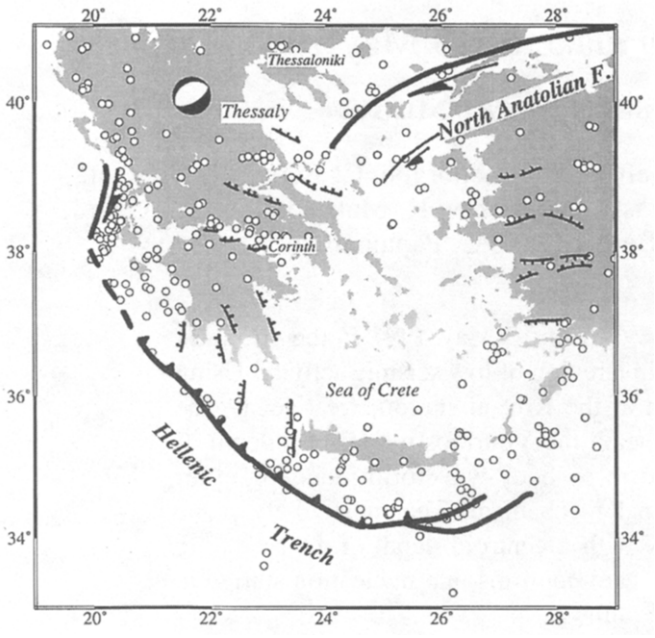

Figure 1. Main tectonic features and seismicity (NEIC, magnitude greater than 4.5 until 1995) of the Aegean. The balloon is the focal mechanism of the Kozani earthquake.

Regional Tectonics and Surface Observations

Kozani is located at the western margin of internal Hellenides in northwestern Greece. Most of the geological structures that form the internal zones of Hellenides trend NW–SE along the Dinarides from Yugoslavia to southern Peloponnese. These NW–SE geological structures experienced extensional tectonics during the Oligocene and late-Miocene time, which produced the Ptolemais–Kozani and Grevena basins. These structures are cut by the ENE–WSW-trending Servia fault, which is one of the most prominent active structures of western Greece. This fault, which is followed by the Aliakmon river, cuts the Miocene and sometimes younger sediments of the Mesohellenic basin. The eastern part is a very important feature showing more than 500-m relief. It bounds the artificial Polyfytos lake and is characterized by steep Holocène fault scarps of about 10 m, attesting to recent activity (Hatzfeld *et al.*, 1995; Meyer *et al.*, 1996). Toward the southwest across the Vourinos massif, the Servia fault continues with the less developed Deskati fault, which is clear on the topography but forms an *en echelon* system offset toward the south (Fig. 2).

Observations of surface breaks conducted after the earthquake did not show any evidence for motion greater than a few centimeters, and discrimination between tectonic ruptures and gravity sliding was not easy (Hatzfeld *et al.*, 1995; Pavlides *et al.*, 1995; Meyer *et al.*, 1996). The best evidence for tectonic surface ruptures was observed south of the Vourinos ophiolite massif, between the villages of Paleohori and Nission. These scarps of a few centimeters of normal slip were located on the Paleohori fault in the continuation of the Servia fault, and therefore north of the Deskati fault. Along the major Servia fault, there were no surface breaks unambiguously related to tectonic features. This statement is supported by the lack of any clear surface rupture across the Aliakmon valley. Open fractures reaching several tens of centimeters and trending E–W were also observed north of the main fault between the villages of Chromion and Grevena (Pavlides *et al.*, 1995). These breaks dipped south and therefore were antithetic to the main fault, but their tectonic origin is questionable, and they could also be caused by gravity sliding.

The Mainshock

Northern Thessaly is a region of low historical seismicity (Papazachos and Papazachou, 1989). The only reported earthquake that could be related to the Servia fault destroyed the city of Veria in 896. The instrumental seismicity record shows low seismicity, occurring mostly after the filling of the artificial Lake Polyfytos (Papazachos *et al.*, 1995) with only one event of magnitude greater than 5 that occurred near Kozani on 25 October 1984.

The mainshock of the Kozani–Grevena earthquake occurred at 08:47 on 13 May 1995 with a magnitude M_s = 6.6. Because it was preceded by five strong (M_s 3.5 to 4.5) foreshocks starting at 08:18 and because of the day of the week (Saturday), most of the public administrative buildings (especially schools) were closed, and no human life was lost even though several villages were almost completely destroyed.

Location

The location of the mainshock computed by the seismological observatory of Thessaloniki is 40.16° N and 21.67° E with a depth of 8.6 km. Due to the lack of stations located close to the epicenter, the accuracy of the location, especially of the depth, is questionable, and we attempt to relocate the mainshock relative to the aftershock sequence using some phases recorded at a local seismological network maintained by Public Power Corporation (PPC).

About 50 strong aftershocks, which were very well located by the local network, are used as sources to compute a mean regional velocity structure that fits the arrival times at the permanent regional stations. We also compute mean residuals for each station that we apply as station corrections to compute the location of the mainshock. Finally, we also use the clear *S-P* travel-time delay of the SMA1 strong-motion instrument located in Kozani, whose minimum value (depending on the trigger delay of the instrument) is 3.4 sec (Fig. 5). When computing the location of the mainshock using only stations with residuals smaller than 2 sec, an inconsistency appears between the seismological station KZN and the strong-motion station SKZ, both located in Kozani. In KZN, we only have the *P* arrival time, whereas in SKZ, we only have the *S-P* arrival delay. Keeping both, we find

a depth of 0.4 km, an rms value of 0.69 sec, and a positive residual of 0.9 sec at SKZ, which seems impossible due to the clear arrival. We eliminate the reading at KZN because we do not thrust the clock and we could not check it ourselves, the depth found is about 13.6 km, the residual is now 0.39 sec in SKZ and 3.6 sec in KZN with a mean rms value of 0.49 sec. We check from well-located aftershocks recorded at SKZ that no important time residual is observed at this station.

The most reliable solution, using the 21 readings whose residuals are smaller than 1.0 sec and excluding the seismological station of KZN, is given in Table 1. The depth is thus 14.2 km, and the mean rms is 0.37 sec. The focus is located underneath the Vourinos ophiolite massif (Fig. 2).

Focal Mechanism

The CMT solution determined by Harvard is a pure normal solution located at a depth of 16 km with one plane trending 240° N and dipping 31° to the NW and the other trending 70° N and dipping 59° toward the SE. We determine some aspects of the rupture process by waveform modeling using 43 very broadband *P* and *SH* waveforms recorded by the GEOSCOPE and IRIS global networks (Fig. 3). Selected *P* waves were at epicentral distances ranging from 30° to 90° and *SH* waves from 30° to 87°. We use the gradient method of Nabelek (1984) to invert the data for centroid depth, mechanism, and source time function. The source time function is constrained to be positive. Theoretical Green's functions of the ray, which include surface-reflected phases, are computed for a simple crustal model with six layers at the source (Rigo *et al.*, 1996) and a single 33-km-thick layer with a *P* velocity of 5.6 km/sec beneath the receivers. We filter the records with a Butterworth bandpass (0.002 to 0.5 Hz) and correct for the instrumental response. In the first step, we invert the *P* and *SH* waves for the best point source mechanism. In a second step, we test the hypothesis of a shock composed of two subevents with independent mechanisms. The data misfit, however, is not improved when allowing for multiple events. We obtain a centroid depth of 11 ± 1 km and a focal mechanism, slightly different from the CMT, that is a normal fault trending 252° ± 1° N and dipping 41° ± 1° to the NW. Figure 3 shows the modeling of the first 20 sec of the signal. The *P*-wave fit is good, whereas the *SH*-wave fit that is nearly nodal and therefore exhibits a smaller signal/noise ratio is not as good. The source time function is dominated by a first large pulse of 6-sec duration followed a few seconds later by another pulse of 8-sec duration, 4 times smaller and not very well constrained. But this second pulse is necessary to improve the misfit. The inversion yields a total scalar moment of 6.2 ×

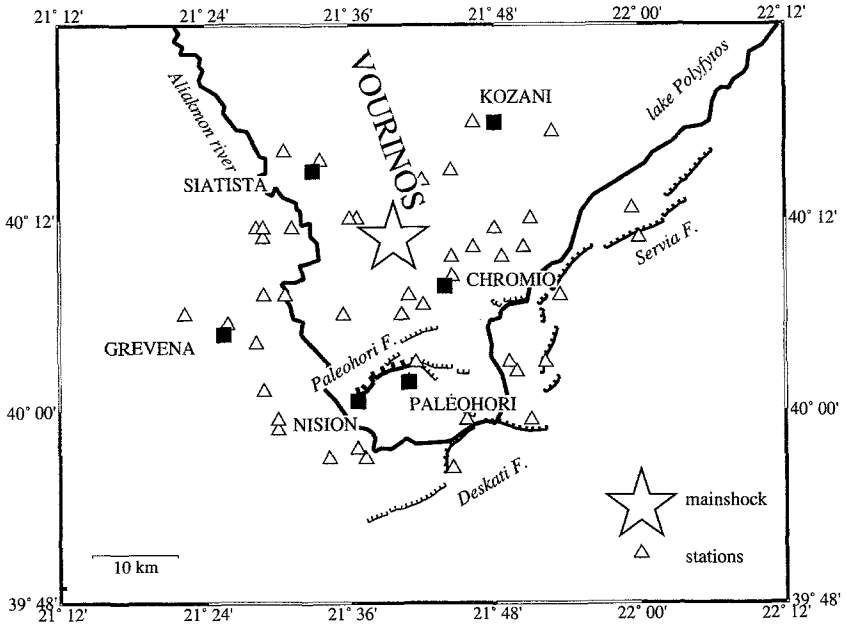

Figure 2. Location map of the temporary network of seismological stations that was installed between 19 May and 25 May 1995. The best solution for the relocated mainshock is indicated by a star. The Servia and Deskati faults are plotted as thin barbed lines, whereas the surface ruptures in Paleohori (Meyer *et al.*, 1996) during the earthquake are plotted as thick barbed line. Solid squares are principal town or villages; triangles are seismological stations.

Table 1
Location of the Mainshock

Date (y/m/d)	Time	Lat	Long	Depth	Mag	No.	rms	ERH	ERZ
95/05/13	8:47:14.58	40–10.95	21–39.58	14.21	6.6	21	0.37	1.8	2.4

Abbreviations: mag, magnitude; no, number of readings; rms, root mean square residuals; ERH and ERZ, uncertainty in epicenter and depth.

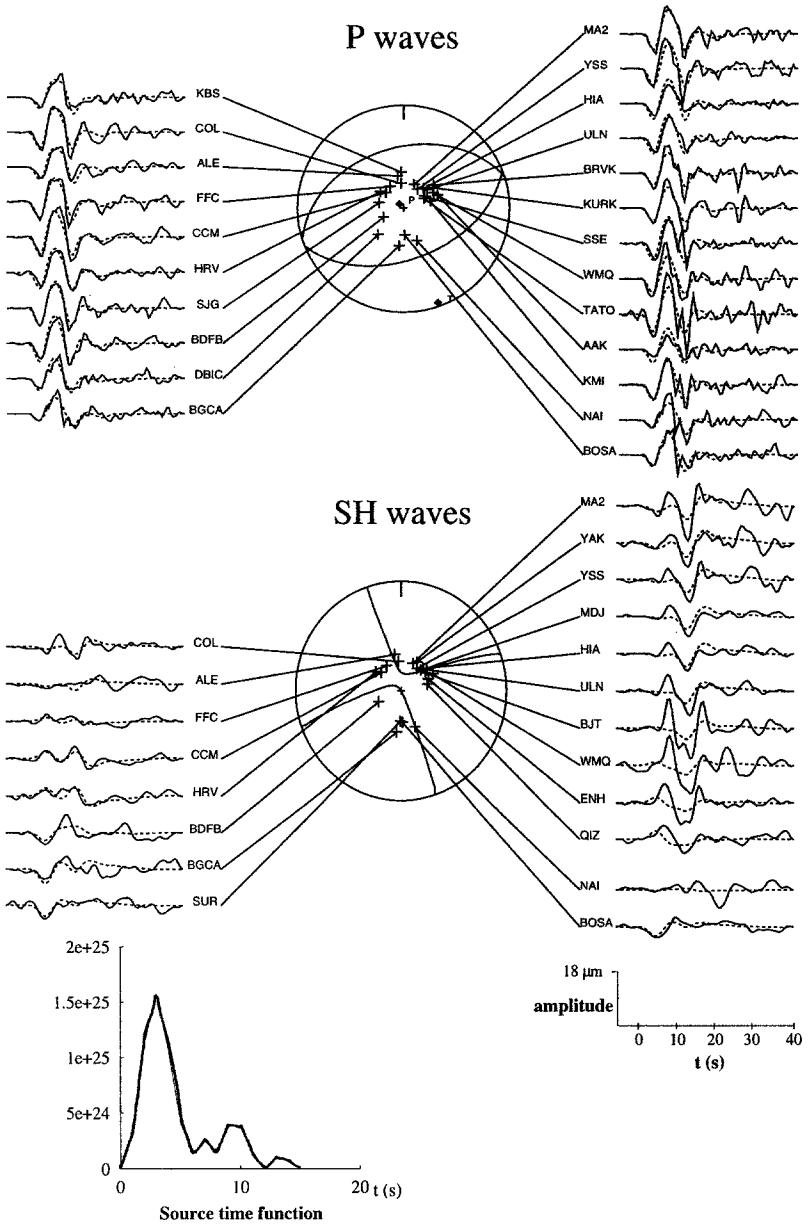

Figure 3. Broadband modeling of *P* and *SH* waveforms at teleseismic distances. The solid line is observed, and the dotted line is the computed displacement. All signals were convolved by a common VBB instrument and filtered with a Butterworth bandpass filter (0.002 to 0.5 Hz). The source time function shows two distinct pulses of 6- and 8-sec duration.

10^{18} N-m, which is smaller than the value of 7.6×10^{18} N-m given by the Harvard CMT. The difference can be explained by the fact that we do not model at the same frequency and use a different velocity structure for the crust. The initial depth given by the short-period instruments is therefore slightly deeper than the centroid depth, suggesting that rupture propagated from the bottom of the fault to the surface.

Rupture Propagation

We use the strong-motion record of the mainshock near the source ($\Delta = 16$ km) to constrain the rupture directivity characteristics. Our synthetic accelerograms are generated in order to match the envelope and the spectral content of the acceleration. We do not try to model velocity or displacement, as the analog record of the SMA1 does not allow safe integration of the signal.

We consider a (26×13)-km fault plane striking 240° N and dipping 40° with a $-85°$ rake (left lateral slip). The lower edge is 15 km deep (Fig. 4); the velocity structure is the same as that used for the locations (Table 1). We define a final dislocation distribution, with a k^{-2} spectral decay, in order to obtain a classical ω^2 source radiation (see Herrero and Bernard, 1994). The slip history is described by a particular source time function, which is wavenumber dependent in order to account for directivity effects (see Bernard *et al.*, 1996). We compute the accelerograms at the Kozani station for four nucleation positions and evaluate only the far-field term of the *P* and *S* direct waves.

Figure 5a presents the E–W component of the acceleration recorded on the SMA1 recorder at Kozani, and Figures

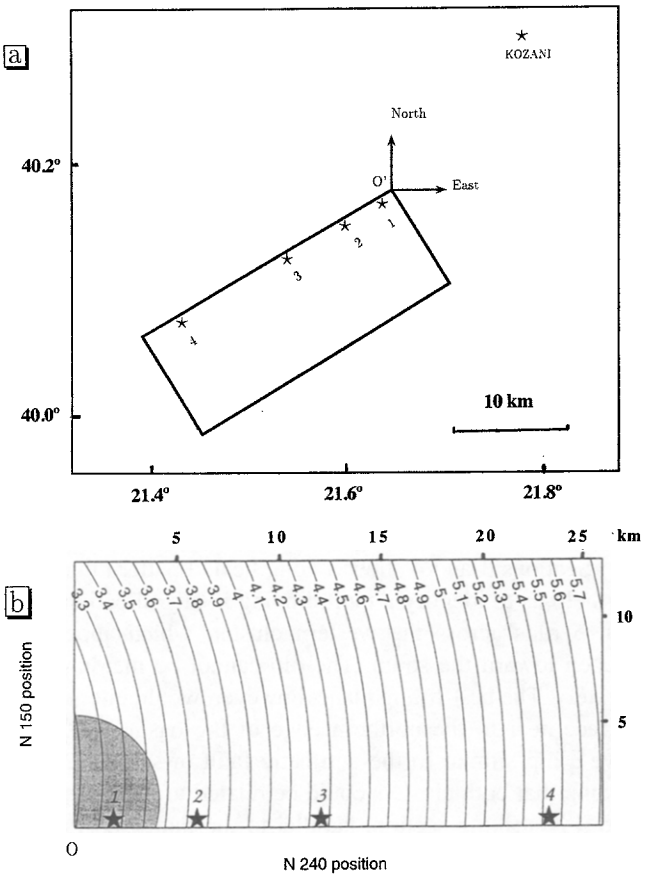

Figure 4. (a) Location of the fault plane used to compute direct *P*- and *S*-wave acceleration at Kozani. The plane is defined by its projection to the Earth's surface. The northern edge is located at 15 km depth. Kozani is located 11.1 km east and 13.3 km north of O'. The stars are different locations for the nucleation. (b) Computation of *S-P* travel times related to different positions for the nucleation point on the main fault plane. The lines represent the *S-P* isochrones at the Kozani station for different hypocenter locations. The shaded circle is the location of the hypocenter in this study with 4 km of associated uncertainty, which fits fairly well with the 3.4 sec isochron. Stars are different locations for the nucleation at the bottom of the fault.

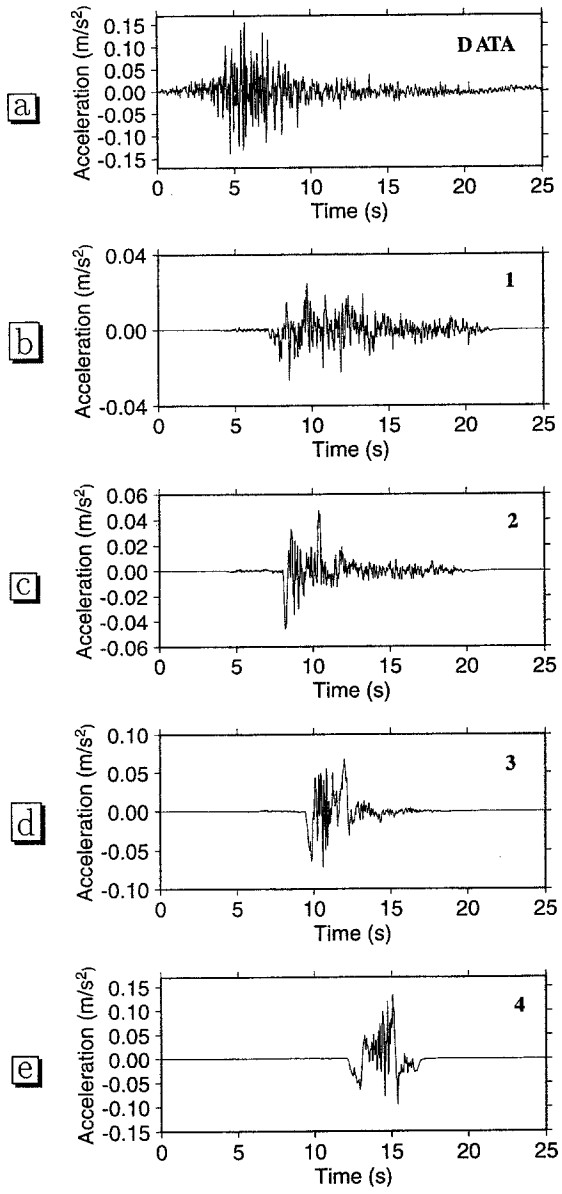

Figure 5. Comparison between observed and modeled accelerations for the E–W component in Kozani. (a) SMA1 record of the E–W component. (b) through (e) Synthetic accelerograms computed for nucleation positions 1 through 4, respectively (see Fig. 4). The best fit is for a nucleation point at location 1.

5b through 5e show synthetic accelerograms for different nucleation positions. The results are roughly the same for the N–S component.

In terms of directivity effects, which control frequency content and signal duration, positions 1 and 2, at the eastern edge of the fault, show a better fit. This is in agreement with the solution proposed by Papazachos *et al.* (1995) and our location. Positions 3 and 4, which make half and more of the fault to be directive for Kozani, produce a low-frequency contribution, which is clearly not observed in the data. The two preferred positions also give a good fit for the *S-P* travel time in the Kozani station. Nevertheless, they do not fit the amplitude of the accelerograms, which may be explained by several factors: the source geometry is most probably much more complicated than our single plane (Meyer *et al.*, 1996); the rupture velocity might be underestimated, and generated higher accelerations due to directivity effects; and finally, site effects at Kozani may also have amplified the ground motion.

Aftershocks

The permanent seismological network is rather sparse in this region. The only station located within 50 km of the

epicenter is Kozani, whose time is questionable and does not allow a precise study of the fault zone. Because this earthquake was the strongest in Greece for the last decade and occurred in an "assumed" aseismic region, we decided to deploy a temporary seismological network of mobile stations made of 15 smoked paper Sprengnether, 10 TAD vertical seismometers, and 15 Lennartz 3D seismometers (Fig. 2). A few strong-motion instruments of various types were also installed. We have already presented the preliminary results from the study of earthquakes recorded by more than eight TAD instruments (Hatzfeld *et al.*, 1995). In this article, we present a more precise study of the same earthquakes, using all 40 available stations to improve the accuracy of the locations computed with HYPO71 (Lee and Lahr, 1972), and we also present the associated focal mechanisms.

We select a set of 50 earthquakes located in a standard velocity structure with a minimum of 24 readings, an azimuth coverage greater than 180°, and an rms value smaller than 0.5 sec. This set was used to compute a V_P/V_s ratio of 1.76, a local velocity structure (Table 2) that minimizes the residuals, and mean station residuals that are applied as station corrections. We relocate the 668 earthquakes that were already recorded by more than eight TAD stations between 19 May and 25 May and select the 622 events that satisfy the following criteria: number of readings greater than 20, rms smaller than 0.15 sec, and uncertainties in both epicenter and depth smaller than 1 km (Fig. 6). The increase of stations as the criterion used to choose among the events allows a more precise view of the seismicity.

The seismicity is concentrated north of the Deskati fault (and therefore west of the Servia fault) and also north of the surface ruptures observed during the mainshock. Most of the activity, with magnitude M 1 between 1 and 3.5, is located between 5 and 15 km depth with a concentration around 8 km. We observe two clusters that are separated by a local minimum of activity. The largest cluster dips roughly to the north. Its lateral dimension of about 20 km is limited by the surface breaks and does not extend more than a few kilometers on either side. It therefore seems reasonable to assume that the mainshock is related to a fault dipping north and consistent with the observed surface breaks. A second cluster, about 10 km wide, is located southwest of the main cluster near the city of Grevena. The depth of the events seems to increase toward the south, in the opposite direction to that of the main cluster.

We compute vertical sections 8 km wide and 7 km apart trending perpendicular to the surface fault across the cluster (Fig. 7). Section 1 is located east of the main cluster, and section 5 crosses the western cluster. On each section, we trace the Deskati fault and the surface breaks along the Paleohori fault when they exist. Section 1 clearly shows a deepening of the aftershocks toward the north from 5 to 15 km. Section 2, which crosses the main cluster, shows a similar pattern of seismicity dipping north with the same angle. According to our relocation, the mainshock is reported at the bottom of the fault plane. We also observe two well-defined clusters, with opposite dip, that are connected to the main cluster at 7 and 10 km depth. The deepest cluster is well defined and looks like an antithetic fault. For these two sections, the dip of the main cluster is about 40° toward the north and would cut the surface approximately around the Deskati fault and therefore south of the surface breaks. The main antithetic branch of section 2 reaches the surface near Siatista in the valley, which cuts the mount Vourinos (Fig. 3).

Table 2
P-Wave Velocity Structure

Velocity (km/sec)	Depth (km)
5.8	0
6.2	8
7.8	30

Sections 3 and 4 show a complicated pattern that does not help us to identify a fault dipping in any direction. Section 5 runs across the western cluster, which appears to deepen toward the south. The dip cannot be measured accurately. The best-fitting plane, however, would intersect the surface near to the northern edge of the basin and would have a dip similar to the antithetic fault of section 2, suggesting that both clusters could be related to the same fault. A 60° N striking section, parallel to the fault, shows three main clusters of activity from west to east: the Grevena cluster, the central cluster, and the eastern cluster (Fig. 7).

We also compute 144 focal mechanisms with a minimum of 20 polarities and an azimuthal gap smaller than 180°. Because our network did not perfectly surround the western cluster, we did not apply the restriction on azimuthal coverage to the western cluster and add 37 more solutions. Most of the solutions are consistent with the mainshock and show normal faulting (Fig. 8). A few solutions are strike-slip motions with a T axis trending roughly NW–SE similar to the normal faulting mechanisms. Most of these strike-slip mechanisms belong to the western cluster. A few mechanisms are associated with the "antithetic" fault seen in section 2. They show the same pattern of normal faulting as the northward-dipping cluster.

Discussion

Now that some characteristics of the mainshock and aftershocks have been described, there are several questions that we wish to address regarding the amount of slip on the fault plane, the geometry of the fault plane related to the surface breaks, and a possible explanation of the antithetic cluster.

The Slip and Surface of the Fault

The static moment of the mainshock given by Harvard is 7.6×10^{18} N-m, whereas the moment computed by body-wave modeling with broadband records is 6.2×10^{18} N-m.

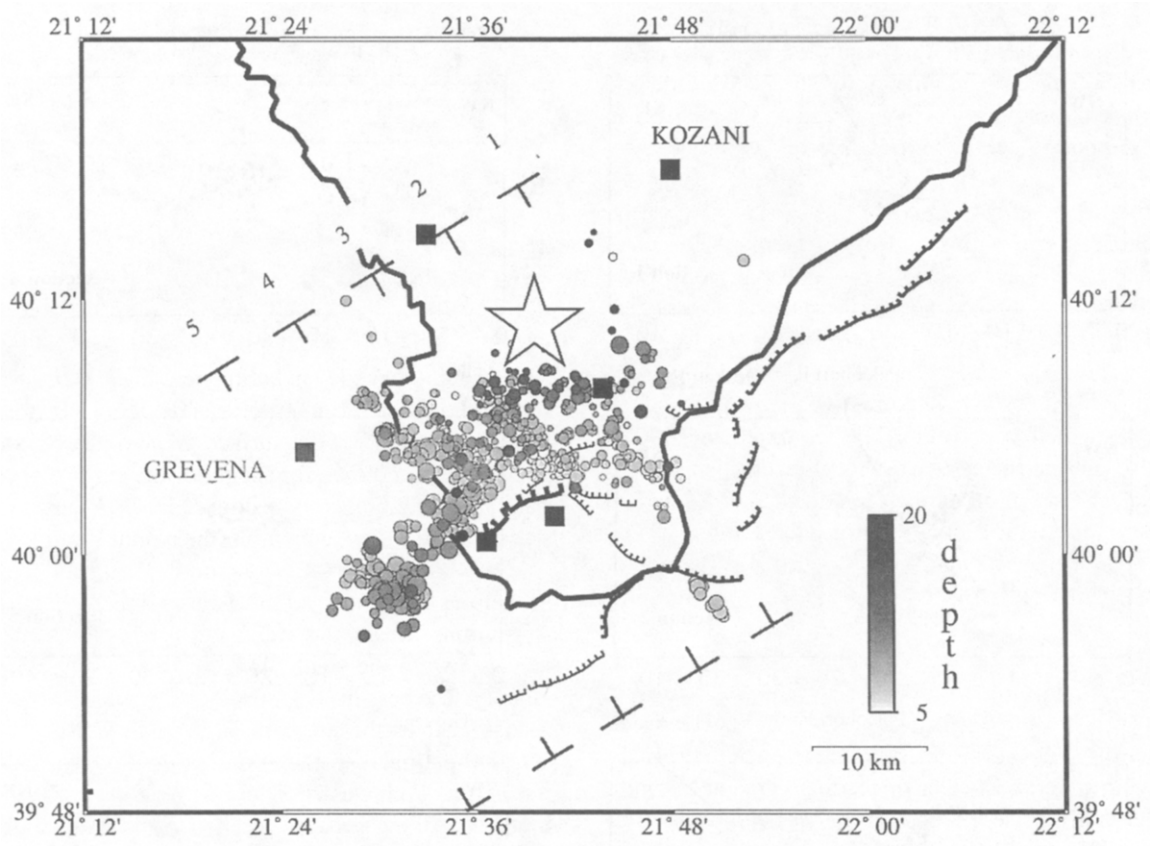

Figure 6. Seismicity map of the 622 aftershocks recorded at more than 20 stations with an rms smaller than 0.15 sec and located with uncertainties smaller than 1 km in terms of both epicenter and depth. Symbols are the same as in Figure 2. The locations of the cross sections are reported.

Given the surface of the fault and, in the case of the Kozani earthquake, that the aftershock seismicity gives the most reliable estimate of the fault surface, we can compute a mean slip on the fault. We can assume that the whole aftershock sequence is related to a single fault going from Grevena to Kozani, which gives a total width of about 35 km, but we can also suppose that the Grevena subcluster is not related to the first pulse of the mainshock, which gives a width of 25 km. The estimate of the length depends on whether or not we assume that the active fault reached the surface, which gives a length of 25 km, or that it was restricted to a depth greater than 5 km, which gives a length of 17 km. The surface area of the fault, therefore, varies from 875 to 425 km^2. We consider this last value as the most probable because aftershocks were restricted to a depth greater than 5 km, the surface breaks were modest, and GPS measurements (Clarke *et al.*, 1996) and Radar Interferometry observations (Meyer *et al.*, 1996; Briole, personal comm.) show that most of the slip is restricted to a plane laterally limited in dimensions. Assuming a rigidity of 3.6×10^{10} Pa, the average displacement on the fault is therefore of 0.5 m. However, it could be 0.25 m if the main fault reached the surface and affected the Grevena cluster, which dips in the opposite direction. This value is slightly less than computed from geodesy.

The Main Fault

At the place where it is clearly defined (sections 1 and 2), the plane that goes through the aftershock seismicity dips at about 35° northward, but the aftershock zone does not reach the surface (Fig. 6). By extrapolation, it is difficult to decide where it cuts the ground surface.

A flat plane of constant dip would cut the surface around the Deskati fault. However, such a shallow dip is uncommon for normal faults and does not fit the observed surface dip of the Deskati fault. Moreover, no surface ruptures were observed on the Deskati fault during the earthquake. Our observations suggest a wider fault plane with a smaller amount of slip. The aftershocks are located on the deepest plane that experienced the largest slip. Finally, we do not have any seismological evidence of a complex fault pattern to the east, as suggested by surface deformation analysis (Meyer *et al.*, 1996). If there is complexity, it should be located on the western part of the fault, around Grevena, where we observe complex seismicity and strike-slip focal mechanisms.

Another possibility is a fault of listric shape fitting the

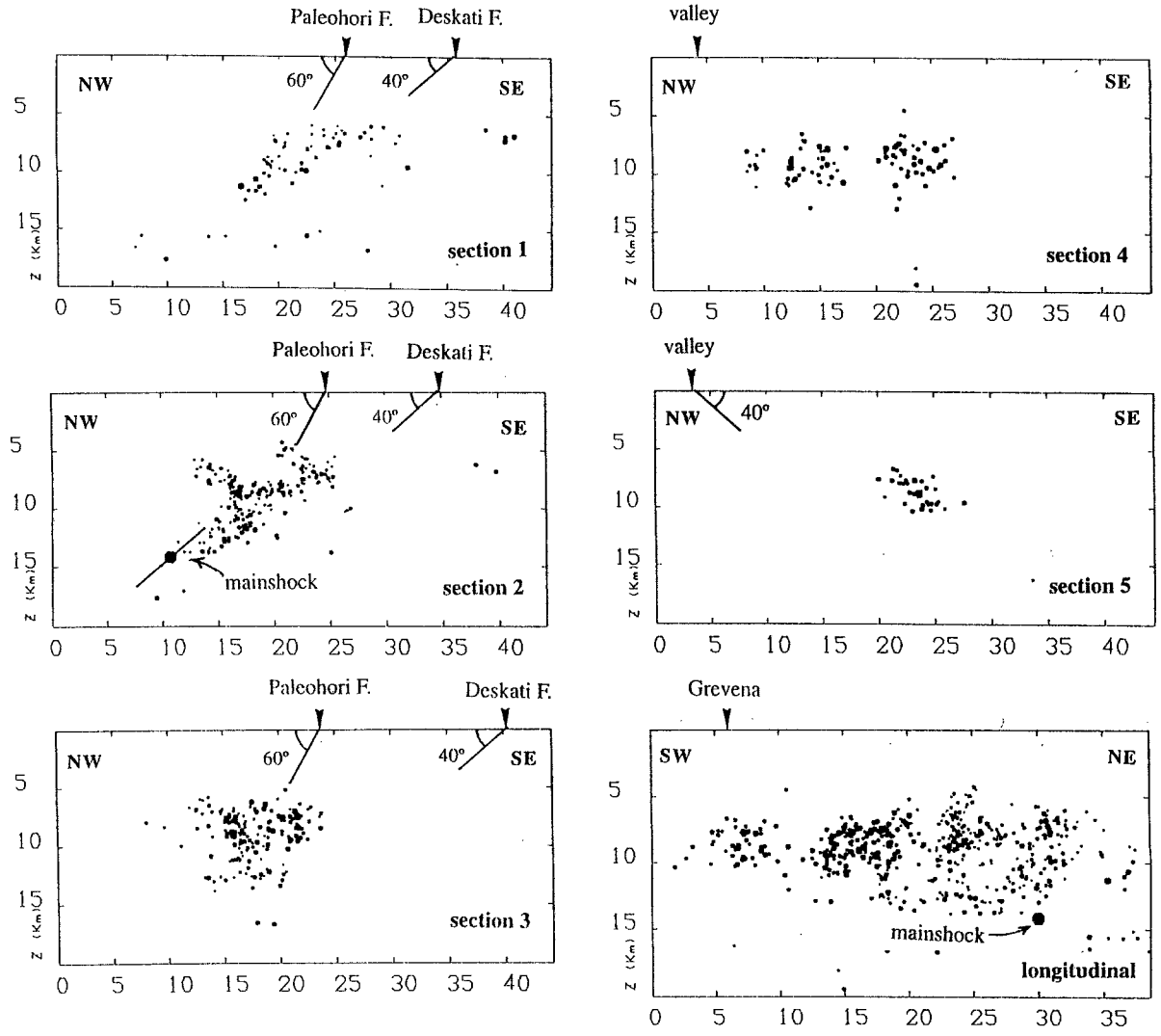

Figure 7. Cross sections trending perpendicular to the surface breaks. The surface traces of the Deskati fault and the ruptures are indicated when available. On some sections, we also indicate the trace of the valley in the Vourinos massif. The mainshock is reported with the dip of the fault plane computed by body-wave modeling.

surface breaks observed in Paleohori and the aftershocks at a depth greater than 5 km. This is similar to the model proposed by Meyer *et al.* (1996) with a 60° dip shallow plane experiencing 1 m of slip, and a 40° dip plane, from 9 to 15 km depth, experiencing 0.4 m of slip.

Our data, however, suggest the active fault plane dipping at 35° to 40° between 6 and 15 km with the upper edge located just beneath the Paleohori surface breaks. In other words, the Paleohori breaks are due to readjustments above the active fault plane.

The Antithetic Cluster

As seen clearly in sections 2 and 5, part of the aftershocks concentrate on a plane that dips southward and is therefore of reverse polarity as compared to the main cluster. Some mechanisms were computed for this cluster and also show normal faulting, striking the same as the main cluster. The extension of this plane reaches the surface in the vicinity of the main road between Kozani and Grevena, near Siatista, where a valley cuts the Vourinos massif.

It is therefore tempting to relate this secondary cluster of activity to an antithetic fault dipping south. An E–W-trending fault, inherited from previous tectonics, was suggested by Vergely (1984) in this region. This antithetic fault is smaller. The approximate dimensions are 8 km in width and 5 km in length, which gives a surface of 40 km^2 that represents about 8% of the main fault surface. This antithetic fault could be the origin of the second pulse in the source time function (Fig. 3), which represents only 15% of the total moment. The slip is therefore of comparable extent for both the main and antithetic faults.

Another possible explanation for this reverse polarity

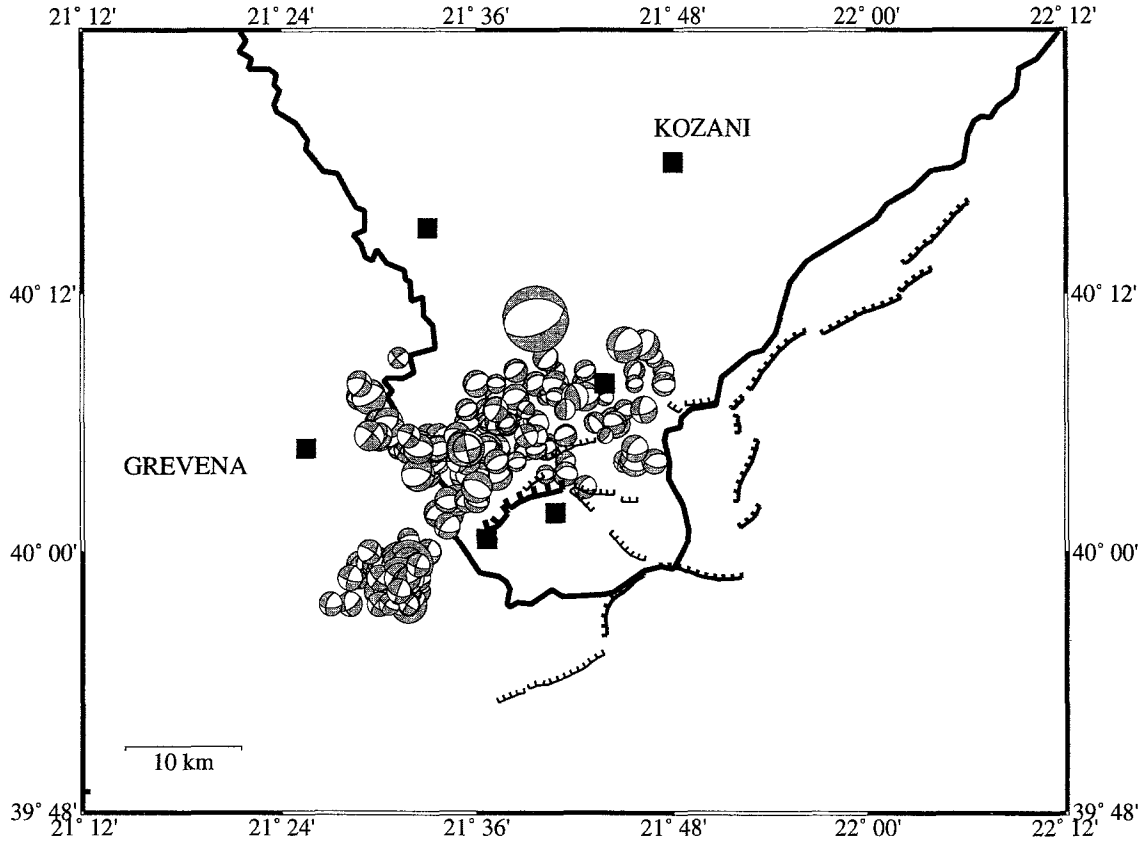

Figure 8. Map of the focal mechanisms computed for the aftershocks. The biggest balloon is the mechanism computed for the mainshock in this study. Most of the aftershocks are normal faulting similar to the mainshock. We observe, however, a few strike-slip solutions, whose *T* axis trends in the same direction as the normal faulting. These strike-slip mechanisms are mostly located to the west of the main cluster.

cluster is a Coulomb stress increase due to the main fault, which helps in triggering aftershocks (King *et al.,* 1994). This pattern of stress change has been used to explain the location of aftershocks and is also considered as a possible mechanism for triggering earthquakes. In our case, however, the "aftershocks" do not branch at an extremity of the fault plane, as should be expected, and we think they are due rather to a secondary fault of smaller dimensions.

A Possible Model

As seen in our seismicity map and cross sections (Fig. 7 and 8), the Kozani earthquake did not rupture one simple plane dipping northward from the surface. In Figure 9, we present a sketch of a possible model.

The mainshock probably occurred on a 40° northward-dipping fault plane, whose upper edge is located at a depth of 5 km beneath Paleohori. This is consistent with the smallness of the surface ruptures and with the co-seismic ground deformation (Briole, personal comm.; Clarke *et al.,* 1996; Meyer *et al.,* 1996). The best candidate for the fault plane is the Deskati fault, but there are several difficulties: We did not observe any surface break on the Deskati fault, shallow-dipping normal faults are uncommon, and the Deskati fault is offset a few kilometers from the main Servia fault. It therefore seems likely that the earthquake ruptured the continuation of the Servia fault. The rupture started on the eastern part and at the bottom of the fault and propagated toward the southwest.

An antithetic cluster offset by a few kilometers toward the southwest is also present. This cluster could be associated with a change in the Coulomb stress due to the mainshock or to an antithetic fault. The well-defined shape of the cluster, the relationship to some topographic changes at the surface, and the presence of a second pulse representing 15% of the total energy released favor an antithetic fault. We have no evidence on the timing of the antithetic fault as compared to the main fault. The only indications we have are the presence of this second pulse on the source time function and that most of the seismic activity was located around Grevena 2 weeks after the earthquake.

This looks like the sequence of the Corinth earthquakes in 1981 (King *et al.,* 1985) where a strong aftershock of magnitude 6.4 ruptured a fault antithetic to the main one. It also resembles the Thessaloniki sequence of 1978 that af-

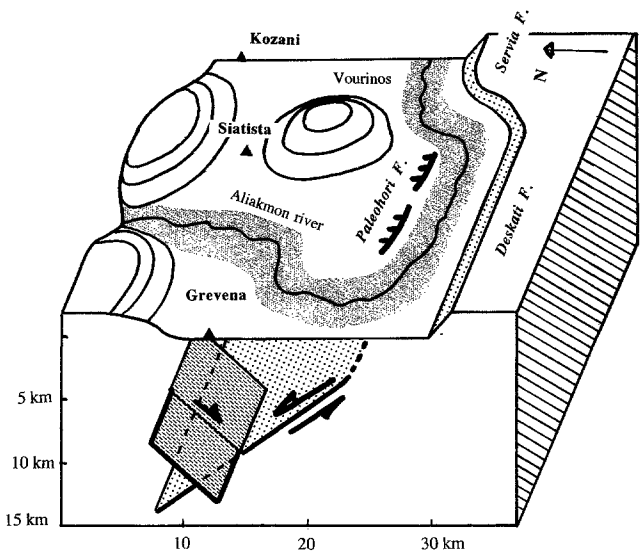

Figure 9. Perspective view of a possible model for the Kozani earthquake. Most of the slip occurred on a fault parallel to the Deskati fault but probably related to the Paleohori surface breaks. This implies a listric shape for the fault, and also that the Paleohori fault is now the active prolongation of the Servia fault. A possible antithetic fault is connected at depth with the main fault.

fected several adjacent segments of the main fault (Soufleris and Stewart, 1981). The offset between the two faults is smaller here than for Corinth or Thessaloniki.

Finally, we have no evidence of any complexity in the aftershocks to the eastern part that could explain a complex pattern of surface deformation (Meyer *et al.*, 1996).

Conclusions

The Kozani earthquake of 13 May 1995 occurred in a region of low seismicity, and it will certainly modify our view of seismic hazards in Greece. It is probably related to the southwestern termination of the Servia fault, a clear active feature that cuts the older geological structures. The mechanism, a normal fault striking 260° N and dipping 40° to the north, is in agreement with the trend of the Servia fault. The *T* axis trends 160° N, which is slightly different from what is observed for the 1978 Thessaloniki earthquakes but consistent with the few available CMT solutions in this area. This orientation therefore supports a slight counterclockwise rotation in the trend of the extension from northern Aegea to western Aegea. The nucleation probably started on the bottom eastern part of the main fault and propagated westward. The aftershock sequence shows a plane dipping 35° northward, which is consistent with the dip given by the mechanism of the mainshock. Seismicity is restricted between 5 and 15 km depth and suggests that slip occurred on a younger fault of listric shape, located north of the Deskati fault. It also suggests that a possible antithetic plane, connected at depth with the main fault and related to the Siatista valley, could be responsible for the second pulse modeled in the source time history. It does not support any complexity in the eastern part of the fault plane.

Acknowledgments

We would like to thank the local authorities for their efficient help during the field work and the PPC of Greece for communicating their data. We had fruitful discussions with R. Armijo, P. Briole, G. King, H. Lyon-Caen, B. Meyer, B. Papazachos, B. Parson, J.-C. Ruegg, D. Sorel, and P. Vergely. Also, B. Meyer, B. Parson, D. Sorel, and P. Vergely critically read a preliminary version of the manuscript, and we benefited from very constructive criticisms from B. Parson, D. Wald, and an anonymous reviewer. J. Nord carefully read the TAD data. This work was supported by the PNRN-INSU program of CNRS, from EC Environment Program, Contracts EV5V-CT94-0413 and EV5V-CT94-0513. One of us (V.K.) was supported during a visit to Grenoble by the Service Scientifique of the French Embassy in Athens.

References

Bernard, P., A. Herrero, and C. Berge (1996). Modeling directivity of heterogeneous earthquake ruptures. *Bull. Seism. Soc. Am.* **86,** 1149–1160.

Clarke, P. J., D. Paradissis, P. Briole, P. C. England, B. P. Parsons. H. Billiris, G. Veis, and J.-C. Ruegg (1996). Geodetic investigation of the 13 May 1995 Kozani–Grevena (Greece) earthquake, *Geophys. Res. Lett.* (accepted).

Hatzfeld, D., J. Nord, A. Paul, R. Guiguet, P. Briole, J.-C. Ruegg, R. Cattin, B. Meyer, A. Hubert, P. Bernard, K. Makropoulos, V. Karakostas, C. Papaioannou, D. Papanastassiou, and G. Veis (1995). The Kozani-Grevena (Greece) earthquake of May 13, 1995, Ms = 6.6. Preliminary results of a field multidisciplinary survey, *Seism. Res. Lett.* **66,** 61–70.

Herrero, A., and P. Bernard (1994). A kinematic self-similar rupture process for earthquakes, *Bull. Seism. Soc. Am.* **84,** 1216–1228.

King, G. C. P., Z. K. Ouyang, P. Papadimitriou, A. Deschamps, J. Gagnepain, G. Houseman, J. A. Jackson, C. Soufleris, and J. Virieux (1985). The evolution of the Gulf of Corinth (Greece): an aftershock study of the 1981 earthquakes, *Geophys. J. R. Astr. Soc.* **80,** 677–693.

King, G. C. P., R. Stein, and J. Lin (1994). Static stress changes and the triggering of earthquakes, *Bull. Seism. Soc. Am.* **84,** 935–953.

Lee, W. H. K. and J. C. Lahr (1972). HYPO71 (revised), a computer program for determining hypocenters, magnitude and first motion pattern of local earthquakes, *U.S. Geol. Surv. Open-File Rept., 75-311.*

Meyer, B., R. Armijo, D. Massonnet, J.-B. de Chabalier, C. Delacourt, J.-C. Ruegg, J. Achache, P. Briole, and D. Papanastassiou (1996). The Grevena (northern Greece) earthquake: fault model constrained with tectonic observations and SAR interferometry. *Geophys. Res. Lett.* **23,** 2677–2680.

Nabelek, J. L. (1984). Determination of earthquake source parameters from inversion of body waves, *Ph.D. Thesis,* Massachusetts Institute of Technology, Cambridge, Massachusetts.

Papazachos, B. and K. Papazachou (1989). *Earthquakes in Greece,* Ekdoseis Ziti, Thessaloniki, Greece, 356 pp.

Papazachos, B. C., D. G. Panagiotopoulos, E. M. Scordilis, G. F. Karakaisis, C. A. Papaioannou, B. G. Karacostas, E. E. Papadimitriou, A. A. Kiratzi, P. M. Hatzidimitriou, G. N. Leventakis, P. S. Voidomatis, K. I. Peftitselis, and T. M. Tsapanos (1995). Focal properties of the 13 May 1995 large (Ms = 6) earthquake in the Kozani area (North Greece), in *Proc. of the XV Congress of the Carpatho-Balkan Geological Association,* Athens, Greece 17–20 September 1995.

Pavlides, S. B., N. C. Zouros, A. A. Chatzipetros, D. S. Kostopoulos, and D. M. Mountrakis (1995). The 13 May 1995 western Macedonia, Greece (Kozani Grevena) earthquake; preliminary results, *Terra Nova* **7,** 544–549.

Rigo, A., H. Lyon-Caen, R. Armijo, A. Dechamps, D. Hatzfeld, K. Makropoulos, P. Papadimitriou, and I. Kassaras (1995). A microseismic study in the western part of the Gulf of Corinth (Greece): implications for large scale normal faulting mechanisms, *Geophys. J. Int.* **126,** 663–688.

Soufleris, C. and G. S. Stewart (1981). A source study of the Thessaloniki (Northern Greece) 1978 earthquake sequence, *Geophys. J. R. Astr. Soc.* **67,** 343–358.

Stiros, S. C. (1995). Unexpected shock rocks an "aseismic area,"! *EOS* **76,** 513.

Taymaz, T., J. A. Jackson, and D. McKenzie (1991). Active tectonics of the north and central Aegean Sea, *Geophys. J. Int.* **106,** 433–490.

Vergely, P. (1984). Tectonique des ophiolites dans les Hellénides internes, conséquences sur l'évolution des régions Téthysiennes occidentales, *Thèse de Doctorat,* l'Université de Paris Sud, Orsay.

Laboratoire de Géophysique Interne et Tectonophysique
IRIGM-CNRS
BP53X
38041 Grenoble Cedex 9, France
(D.H., R.G., A.P.)

Geophysical Department
Aristotle University
BP 352-1
540-06 Thessaloniki, Greece
(V.K., P.V.)

Seismological Laboratory
University of Athens, Illissia
15784 Athens, Greece
(M.Z., D.D., I.Ka., I.Ko., K.M.)

Istituto Nazionale di Geofisica
via di Vigna Murata 605
00143 Roma, Italy
(G.S., R.A., M.DiB., S.B.)

Département de Sismologie
Institut de Physique du Globe
CNRS, Case 89
75252 Paris Cedex 05, France
(S.L., C.B., P.B.)

ITSAK
P.O. Box 53
Finikas
55102 Thessaloniki, Greece
(C.P.)

Manuscript received 18 March 1996.